



HAL
open science

Voltage Control Based on a Non-Linear Load Observer for Synchronous Reluctance Generator

Laurent Schuller, Romain Delpoux, Jean-Yves Gauthier, Xavier Brun

► **To cite this version:**

Laurent Schuller, Romain Delpoux, Jean-Yves Gauthier, Xavier Brun. Voltage Control Based on a Non-Linear Load Observer for Synchronous Reluctance Generator. ECC 22, Jul 2022, London, United Kingdom. 10.23919/ECC55457.2022.9838259 . hal-03629067

HAL Id: hal-03629067

<https://hal.science/hal-03629067>

Submitted on 4 Apr 2022

HAL is a multi-disciplinary open access archive for the deposit and dissemination of scientific research documents, whether they are published or not. The documents may come from teaching and research institutions in France or abroad, or from public or private research centers.

L'archive ouverte pluridisciplinaire **HAL**, est destinée au dépôt et à la diffusion de documents scientifiques de niveau recherche, publiés ou non, émanant des établissements d'enseignement et de recherche français ou étrangers, des laboratoires publics ou privés.

Voltage Control Based on a Non-Linear Load Observer for Synchronous Reluctance Generator

Laurent Schuller* *IEEE Student Member*, Romain Delpoux[†], Jean-Yves Gauthier[‡] and Xavier Brun[§]
Univ Lyon, INSA Lyon, Université Claude Bernard Lyon 1, Ecole Centrale de Lyon, CNRS, Ampère, UMR5005
69621 Villeurbanne, France

Email: *laurent.schuller@insa-lyon.fr, †romain.delpoux@insa-lyon.fr,
‡jean-yves.gauthier@insa-lyon.fr, §xavier.brun@insa-lyon.fr

Abstract—This paper proposes a voltage control law based on the parameter estimation of a resistive load via a non-linear observer. The main benefit of the proposed observer is to show a dynamic of convergence independent of the state value. Simulations and experimental verifications are performed in order to verify the effectiveness of the controller and the observer.

Index Terms—Synchronous Reluctance generator, parameter estimation, non-linear observer.

I. INTRODUCTION

The electrical machines were responsible of between 43% and 46% of the global electricity consumption in 2011 [20]. This part tend to extend in the future years due to the electrification that has been considered as one way to reduce the pollution problem by replacing diesel or hydraulic actuator by electrical machines. In this context, the synchronous reluctance machine (SynRM) technology gain more and more interest since a few years [4]. This is explained on the one hand by the ecological and economic issues that force constructors to use less rare-earth magnets [8] [2]. On the other hand, advances in power electronics and new SynRM designs [15] made the machines more efficient. Nowadays, the SynRM challenges the traditional induction machine (IM) in various applications such as the electrical vehicles [1], [18], [21] or industrial applications [9]. Thanks to its lower weight and its enhanced efficiency, the SynRM is the most likely candidate to replace aging IM in industrial plants.

Due to the electromagnetic conversion reversibility, the SynRM as most of electrical machines can be used as a motor or a generator. In this paper, we are interested into a system that involves a SynRM generator using an active rectifier as in [7] and [6] except that we consider a SynRM instead of the IM. The system is considered for an off-grid electric power generation application. In the cited studies, the authors proposed a voltage control law based on a linearisation of the DC voltage dynamic around an equilibrium point. The controller's performances are then locally but not globally ensured. A similar system has been investigated in [10] where the DC voltage regulation was also based on a Proportional Integral (PI) controller. The DC voltage control of an AC/DC Pulse width modulation (PWM) converter via a feedback linearisation has been studied in [11]. In the

latter, the load current was measured via a physical sensor. In all the cited studies, the proposed tuning methods for the controllers require physical parameters. It is then necessary to estimate them. The problem of parameter estimation has been investigated since decades. Among the various methods developed to estimate parameters, the simplest way is to measure the parameters before the system operates. Another possibility is to set up an identification procedure that can be either offline [17] or online [13]. During an offline identification procedure, the normal operation of the system is not guaranteed. In addition, if the parameter changes during operation, its prior measurement and offline identification are obsolete and the change is not detected. This leads to a miss estimation of the parameter. On the contrary an online estimation procedure allows the system to operate normally and to estimate the parameter simultaneously. Thereby, any change in the parameter value is detected and its estimation is updated as it is the case for the recursive least square method [19]. However, the system operation is often slightly altered as it is the case when high frequency injections are employed [22]. Finally, the parameter can be derived from an observer provided the dynamic model of the system is known. In this case, the operation of the system is not affected and any change is detected. A general theory about the non-linear parameters observation is proposed in [5]. The observed parameters can be used in the control loop in order to improve the robustness or the dynamic performances of the controller. In that sense, in [14] the author used an extended Kalman filter in order to observe the inductances, winding resistance and iron losses equivalent resistance of a machine. All these observations are used in the control to improve the performances of the system. More generally, in [3] an overview of the methods used to estimate the disturbances and their uses in the control is proposed.

In this paper, we aims to develop a global DC voltage control law based on the observation of the equivalent resistive DC load. This is motivated by the important variations that may occur for this parameter during operation. This parameter estimation is considered with the intention of getting rid of the load current sensor.

The paper is structured as follows: in section II the considered system is detailed and the objective of the paper

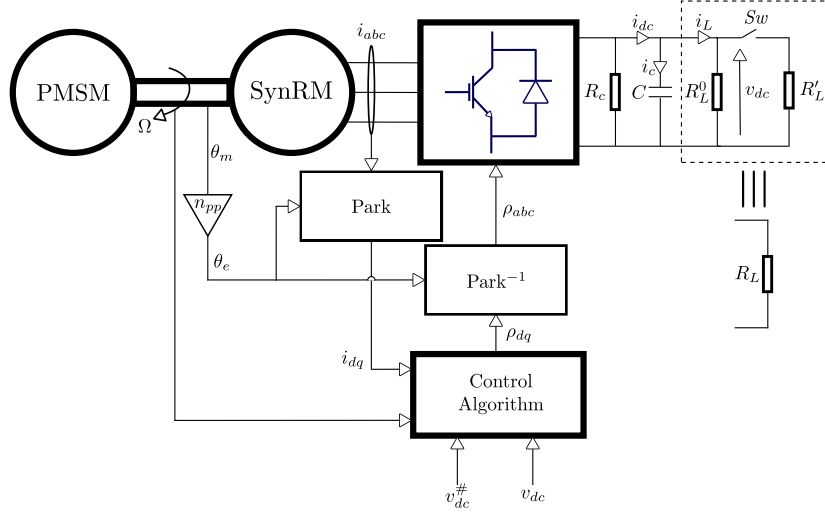


Fig. 1. Schematic representation of the considered system

is explained; In section III, the proposed control strategy is presented and the necessity of a resistive load observer is underlined; In section IV, the proposed non-linear parameter observer is explained and the closed loop behaviour is shown. Simulations are performed in section V in order to verify the proper operation of the proposed control law based on the load observer. The experimental verification is performed in section VI; Finally the perspectives and conclusion are given in section VII.

II. PROBLEM STATEMENT

This work considers the SynRM as a generator. The generator is driven by a three-phase 2-levels AC/DC converter. The control objective is to regulate the v_{dc} voltage to its positive reference value $v_{dc}^{\#}$. The considered system is shown schematically on Fig.1.

The Park transform [16] is used in order to project the classical three-phase frame (a, b, c) into the (d, q) rotating frame. Thus, the three-phase currents i_{abc} and duty cycles ρ_{abc} are projected on their (d, q) counterparts, namely i_{dq} and ρ_{dq} . This projection requires the electrical position θ_e of the machine. The mechanical position θ_m is measured using an incremental encoder. Using n_{pp} , the machine pole pairs number, one has $\theta_e = n_{pp}\theta_m$. The dynamical model of the SynRM's electrical behaviour is given by:

$$L_d \frac{di_d}{dt} = \rho_d v_{dc} - R_s i_d + n_{pp} L_q \Omega i_q, \quad (1a)$$

$$L_q \frac{di_q}{dt} = \rho_q v_{dc} - R_s i_q - n_{pp} L_d \Omega i_d, \quad (1b)$$

$$C \frac{dv_{dc}}{dt} = -\frac{3}{2} (\rho_d i_d + \rho_q i_q) - \frac{1}{R_L} v_{dc} - \frac{1}{R_c} v_{dc}, \quad (1c)$$

where L_d, L_q are the inductances of the machine in the Park rotating frame. The rotational speed is noted Ω . The variables ρ_d and ρ_q represent the duty cycles in the Park reference frame. The parameter R_s is the stator resistance.

A resistive load R_L^0 is connected to the DC bus. The converter losses are modeled by an equivalent resistor R_c in parallel of the capacitor C [23]. The value of R_c depends widely on the operating point. To simulate a load variation, an additional load R_L^1 can be inserted via a switch Sw during the operation of the generator. In the rest of this paper, the total resistive load $R_T = \frac{R_c R_L}{R_c + R_L}$ is often considered. All these components necessarily have strictly positive values. In this article we consider a positive initial voltage at the capacitor C terminals leading to a positive initial DC voltage.

To ensure positive and constant speed of the generator, a permanent magnet synchronous motor (PMSM) is connected to the shaft of the SynRM generator.

The objective of this work is to ensure constant DC voltage at the capacitor terminals despite unknown load variations. It is assumed that the states and the control variables are measured and therefore are available for the use in the design of the control law.

III. CONTROL STRATEGY

The considered system is composed of two subsystems with different dynamics. In the model represented by the system (1), the two first equations (1a) and (1b) represent the fast current dynamics. The last equation (1c) represents the slower voltage dynamic. This time scale separation motivates the consideration of cascaded control loops composed by a fast inner loop for the currents control and a slower outer loop for the voltage. The Fig. 2 shows the control scheme with the cascaded controllers.

The objective of the inner current loop is to ensure that, at steady state, the current references are reached by the measured currents, leading to zero steady state error. Generally, a field oriented current controller [12] is used for this purpose. Outside the magnetic saturation zone, a classical choice for SynRM is to track $i_q = -|i_d|$. This condition minimises the ohmic losses for a given torque production. Maintaining a

fast closed loop dynamic, one can consider currents at steady state compared to voltage dynamic. The currents steady states are deduced from:

$$\rho_d^* = \frac{1}{v_{dc}}(R_s i_d^* - n_{pp}\Omega L_q i_q^*), \quad (2a)$$

$$\rho_q^* = \frac{1}{v_{dc}}(R_s i_q^* + n_{pp}\Omega L_d i_d^*). \quad (2b)$$

where $(\cdot)^*$ denotes the variable (\cdot) at steady state.

Combining (2) with (1c), the slower voltage dynamic can be rewritten as:

$$\frac{dv_{dc}}{dt} = -\Lambda \frac{i_d^{*2}}{v_{dc}} - \frac{1}{R_T} \frac{1}{C} v_{dc}, \quad (3)$$

where Λ is defined as:

$$\Lambda = \frac{3}{2C} (2R_s + n_{pp}\Omega(L_q - L_d)sgn(i_d)). \quad (4)$$

The sign function given by:

$$\begin{cases} sgn(x) = -1 & \text{if } x < 0, \\ sgn(x) = 1 & \text{else.} \end{cases} \quad (5)$$

In equation (3) i_d^* can be considered as a control variable. It is chosen as in equation (6) where $\pm\sqrt{\cdot}$ is the signed square root function defined in (7). In this way, the resistive load effect is compensated and the closed loop voltage dynamic is arbitrarily chosen while making sure to stay significantly slower than the fast inner loop.

$$i_d^* = \pm\sqrt{-\frac{v_{dc}}{\Lambda} \left(\frac{1}{R_T} \frac{1}{C} v_{dc} - g(v_{dc} - v_{dc}^\#) \right)}, \quad (6)$$

where $v_{dc}^\#$ is the voltage reference and g is a positive parameter to be chosen.

$$\pm\sqrt{x} = \sqrt{|x|}sgn(x) \quad (7)$$

Combining (6) with (3) gives the closed loop slower voltage dynamic behaviour:

$$\frac{dv_{dc}}{dt} = -g(v_{dc} - v_{dc}^\#) \quad (8)$$

Noting that $|n_{pp}\Omega(L_q - L_d)| \geq 2|R_s|$ is required for the normal operation of the system and $i_d^* i_d^* \geq 0$, one can express $sgn(i_d^*)$ without needing to know i_d^* . The two equations (4) and (6) are thus not implicit.

The proposed control law (6) requires a good knowledge of the system. As a simplification, we consider most of the parameters as constant during operation. The number of pole pairs n_{pp} is obviously constant. Neglecting the thermal behaviour by considering an almost constant temperature leads to assume the parameters R_s and C constant. This assumption is feasible when the currents are not large enough to significantly warm the coils by Joule heating. Finally, outside the magnetic saturation zone, the inductances L_d and L_q are constant. Finally, in our study, the major uncertainties in (6) concern the value of the total resistive load R_T . Not only the value of R_L may change during the operation via

the activation of the switch "Sw". But also the converter losses represented by the resistor R_c are highly dependant of the operating point and can change significantly.

The next section aims to develop a non-linear parameter observer in order to estimate the quantity $\frac{1}{R_T}$ online.

IV. NON-LINEAR OBSERVERS

Because the parameter R_T only appears in the last equation (1c) of system (1), we consider solely this equation for the further developments. Consider the change of variables:

$$\begin{aligned} u &= \frac{3}{2}(\rho_d i_d + \rho_q i_q), \\ \theta &= \frac{1}{R_T}, \end{aligned} \quad (9)$$

where the unknown parameter θ is supposed to be constant. Thus, equation (1c) is transformed into:

$$\begin{cases} \dot{x} &= -\frac{1}{C}(u + \theta x), \\ \dot{\theta} &= 0. \end{cases} \quad (10)$$

In [5], a general expression for non-linear parameter observers in the multi-variables case for dynamical system is given as:

$$\dot{x} = h(x, u, \theta), \quad (11)$$

where $h(x, u, \theta)$ is a possibly non-linear function. The general expression of a non-linear parameter observer is given by (12).

$$\begin{cases} \dot{\hat{\theta}} &= \phi(x) + \zeta, \\ \dot{\zeta} &= -\Phi(x)h(x, u, \hat{\theta}), \end{cases} \quad (12)$$

where $\phi(x)$ is an appropriately chosen nonlinear function and $\Phi(x)$ is its Jacobian matrix.

A. Existing observer

This general method can be applied for the model (10). As proposed in [5], a function $\phi_1(x)$ is chosen as:

$$\phi_1(x) = -K_1 x^2, \quad \text{with: } K_1 > 0. \quad (13)$$

From this function and its derivative with respect to x , the non-linear observer is obtained as:

$$\begin{cases} \dot{\hat{\theta}} &= -K_1 x^2 + \zeta, \\ \dot{\zeta} &= -2\frac{K_1}{C} x u - 2\frac{K_1}{C} \hat{\theta} x^2. \end{cases} \quad (14)$$

For the observer (14), the evolution of the error of observation $e_1 = \hat{\theta} - \theta$ is expressed as follows:

$$\begin{aligned} \dot{e}_1 &= \dot{\hat{\theta}} - 0 \\ &= -2\frac{K_1}{C} x^2 e_1. \end{aligned} \quad (15)$$

The dynamic of the observer error e_1 depends on the state x value. Generally speaking, it is preferable to obtain a convergence rate for the observer which is independent of the state x .

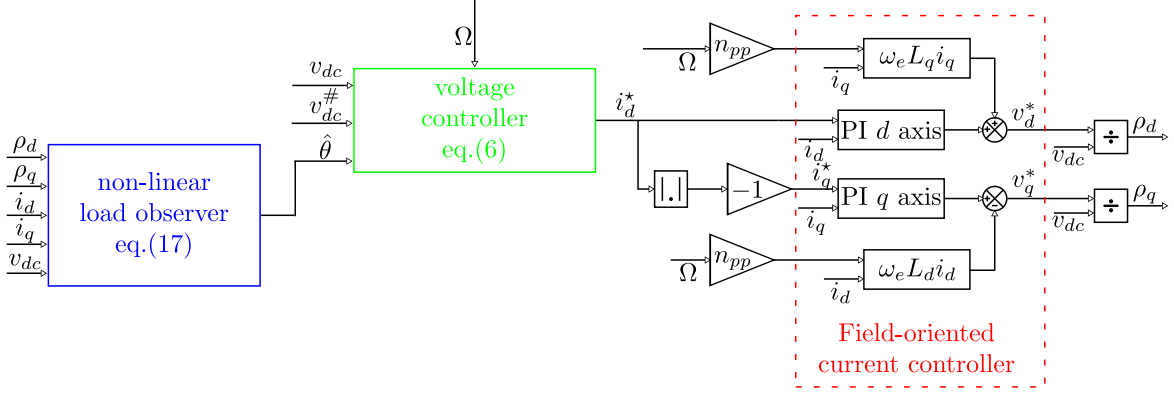


Fig. 2. Control scheme

B. Proposed non-linear parameter observer

As the author explained in [5], the choice of the function $\phi(x)$ is not unique. It is desirable to obtain an observer's error of the form $\dot{e}_2 = -ke_2$ with $k > 0$. In order to drive the error of the observer asymptotically to zero with a dynamic independent of x , we propose a new function $\phi_2(x)$. Let us remember that the state x is scalar and strictly positive.

$$\phi_2(x) = -kC \ln(x), \quad \text{with: } k > 0. \quad (16)$$

The proposed non-linear observer is then expressed as:

$$\begin{cases} \dot{\hat{\theta}} = -kC \ln(x) + \xi, \\ \dot{\xi} = -k \left(\frac{u}{x} + \hat{\theta} \right). \end{cases} \quad (17)$$

The error $e_2 = \hat{\theta} - \theta$ of the proposed observer (17) is governed by the following equation:

$$\begin{aligned} \dot{e}_2 &= \dot{\hat{\theta}} - 0, \\ &= -kC \frac{\dot{x}}{x} - k \left(\frac{u}{x} + \hat{\theta} \right), \\ &= -k(\hat{\theta} - \theta), \\ &= -ke_2. \end{aligned} \quad (18)$$

C. Observer based control

By replacing the parameter $\frac{1}{R_T}$ in (6) by its observation $\hat{\theta}$ from (17) one can determinate the closed loop behaviour. The tracking error is introduced as $\widetilde{v}_{dc} = v_{dc} - v_{dc}^\#$. Because the DC voltage reference $v_{dc}^\#$ is piecewise constant, the derivative of the tracking error is expressed as $\dot{\widetilde{v}}_{dc} = \dot{v}_{dc}$.

$$\begin{cases} \dot{\widetilde{v}}_{dc} = \frac{1}{C} e_2 \widetilde{v}_{dc} - g \widetilde{v}_{dc} + \frac{1}{C} e_2 v_{dc}^\#, \\ \dot{e}_2 = -ke_2, \end{cases} \quad (19)$$

If the observer converges faster than the controller, the stability of (19) should be ensured. The evolution of the observer error is expressed as:

$$e_2(t) = e_0 \exp(-kt), \quad (20)$$

where e_0 is the initial observer error and $\exp(\cdot)$ is the exponential function. From there, the tracking error can be deduced as:

$$\begin{aligned} \widetilde{v}_{dc}(t) &= v_0 \exp(A(t=0)) \exp(-A(t)) \\ &\quad + v_{dc}^\# \int_0^t \exp(A(s)) ds \exp(-A(t)) - v_{dc}^\#, \end{aligned}$$

with: $A(t) = gt + \frac{1}{kC} e_0 \exp(-kt)$, (21)

where v_0 is the initial DC voltage. The stability of the system is deduced from the expression (21) under the condition of positive values for the parameters g and k .

V. SIMULATION VERIFICATION

The proposed controller (6) and non-linear observer (17) are verified in simulation. For these simulations, the inductances L_d and L_q are chosen constant. The initial conditions are chosen as follow:

$$\begin{aligned} v_{dc}(t=0) &= 100V, \\ i_d(t=0) &= 0.35A, \\ i_q(t=0) &= -0.35A, \\ \xi(t=0) &= 0. \end{aligned} \quad (22)$$

From this initial point, the voltage reference is firstly increased to 135V. Afterwards, a load step is applied, making the load going from 11 k Ω to 300 Ω . The parameter g is chosen equal to 2 and k is equal to 25. The SynRM's parameters are the same as those of the experimental setup, their values are given in section VI. The results are shown on Fig. 3. After a quick initialisation, the parameter observer converges and the voltage reaches its reference. The voltage follows its reference with the desired dynamic. During the load step, the parameter observer converges rapidly enough so that the voltage stay close to its reference. After a very short time, the perturbation is almost completely rejected. During the reference changes (at 3s and 9s) the DC voltage v_{dc} variation is limited by the controls saturations. Indeed, the control inputs ρ_d and ρ_q are constrained such that $\rho_d^2 + \rho_q^2 < Cst$, where Cst is a positive constant whose value depends on

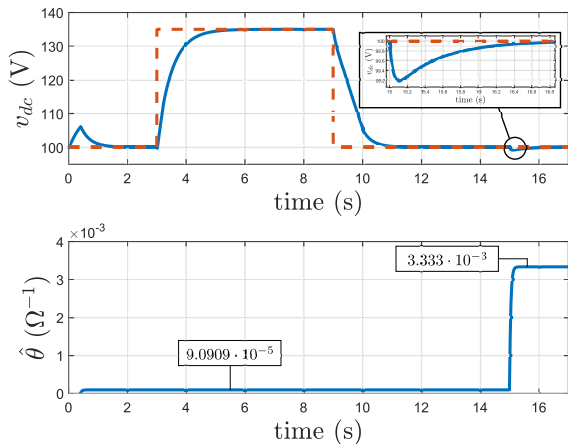


Fig. 3. Simulation results, evolution of v_{dc} on the upper graph (red dashed line: reference, blue solid line: measurement) and the parameter observation on the lower graph

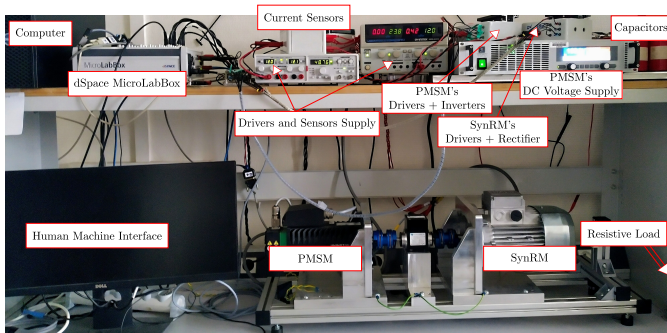


Fig. 4. Experimental test bench

the PWM (Pulse Width Modulation) technique chosen. A conservative manner of dealing with this is to saturate the current reference i_d^* . This option has been adopted for the presented simulation.

VI. EXPERIMENTAL APPLICATION

A. Presentation of the experimental setup

The diagram represented in Fig. 1 is carried out experimentally. Fig. 4 shows a photograph of the test bench we used for the experimental verifications. For the experimental tests, a BSR90LE154055FB5 SynRM from Bonfiglioli is used. Its main characteristics are listed in Table I. A Leroy-Somer 95UMC300HAAAA PMSM with the same speed and power range is attached to the SynRM by the shafts. Both machines are fed through three-phase converters composed of NTHL080N120SC1 SiC MOSFET. Position and speed measurements are provided by an incremental encoder with 5000 points per mechanical revolution. All acquisitions are extracted through a dSpace MicroLabBox Rapid Control Prototyping (RCP) System. The sampling time (10^{-4} s) is chosen small enough compared to the dynamics of the system. The latter is then considered continuous.

TABLE I

MAIN PARAMETERS OF THE SYNCHRONOUS RELUCTANCE MACHINE

Parameters	Value	Units
Base speed (mechanical) Ω_m	157	rad/s
Number of pole pairs n_{pp}	2	—
Rated current I_n	4.5	A
Power P_n	1500	W
Nominal phase voltage V_n	230	V
Resistance per phase R_s	2.6	Ω

B. Control of the system

The dynamics of the currents and the DC voltage are distant enough to consider a control strategy based on cascade controllers. The whole experimental control scheme is shown on Fig. 2.

C. Experimental verifications

A first experiment aims at highlighting the difference between the two observers. For this purpose, only the currents controller is used to drives the currents i_d and i_q to their references which are namely $0.39A$ and $-0.39A$. In these conditions, the DC voltage reaches about $135V$. While the currents are regulated at their references, a manual switch "Sw" is turned on making the resistive load R_L go from $11k\Omega$ to $2.2k\Omega$. The load variation is estimated by the two observers expressed in (14) and (17). The parameter k in (17) is chosen equal to 25. The parameter K_1 in (14) is chosen equal to $1.2551 \cdot 10^{-6}$ in order to show similar convergence rate to that of the other observer when the operating point is around $v_{dc} = 135V$. The same procedure is repeated with smaller current references leading to lower initial voltage of $100V$. During this experiment, the DC voltage changes since only the currents are regulated and the resistive load is modified. If the voltage variation is too large, meaning the voltage value drops close to a too low value, the normal operation is no longer guaranteed. Indeed the control variables are actually bounded, the proposed modelling does not take this into account, the developments of this paper only concern an unsaturated system. To prevent the saturation issue, the additional load R'_L is chosen such that the overall load R_L is equal to $2.2k\Omega$ instead of 300Ω as it is the case for other experiments. Despite the voltage variation is slower than the observers convergence, it does have a small effect on the observer convergence time. The results are shown on Fig. 6. From that figure, it can be seen that the observer (17) shows the same convergence rate for the two operating points. On the opposite, the observer (14) shows different convergence time.

Remark 1. The capacitor value appears in the observers equations, this value is not expected to change significantly. Hence, an attention has been paid to its measurement before the system is put into operation. The capacitor value is $C = 1.83 mF$

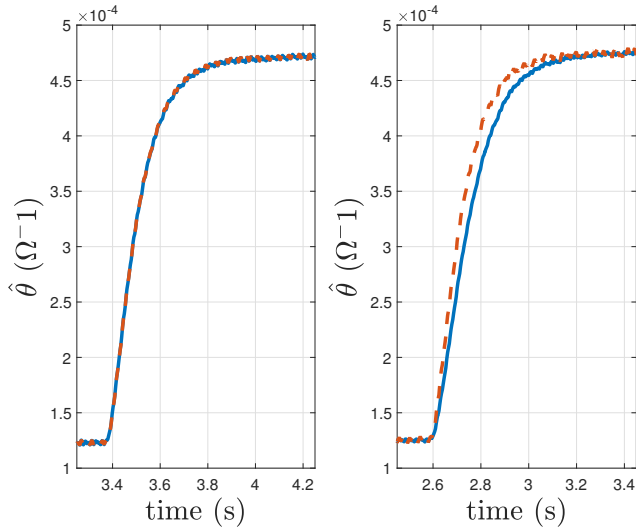


Fig. 5. Comparison of the two observers (blue solid line (14) and red dashed line (17)) for two different operating points (around $v_{dc} = 135V$ for the graph on the left and around $v_{dc} = 100V$ for the graph on the right)

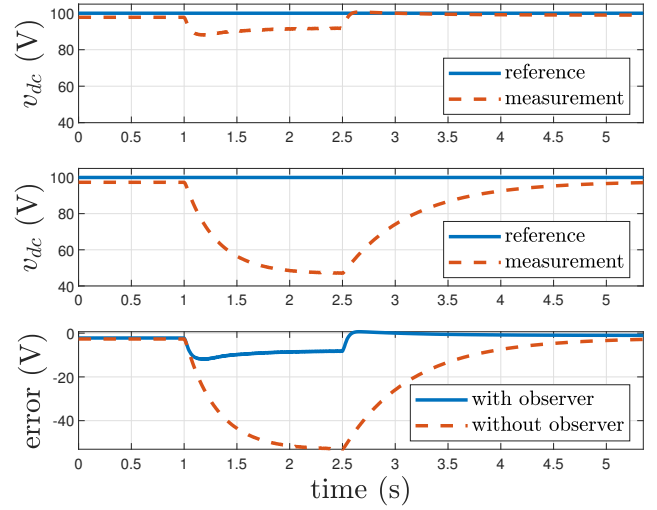


Fig. 7. Regulation of v_{dc} with the observed parameter compensation (up), without the observed parameter compensation (middle) and comparison of the error $v_{dc} - v_{dc}^{\#}$ for both cases

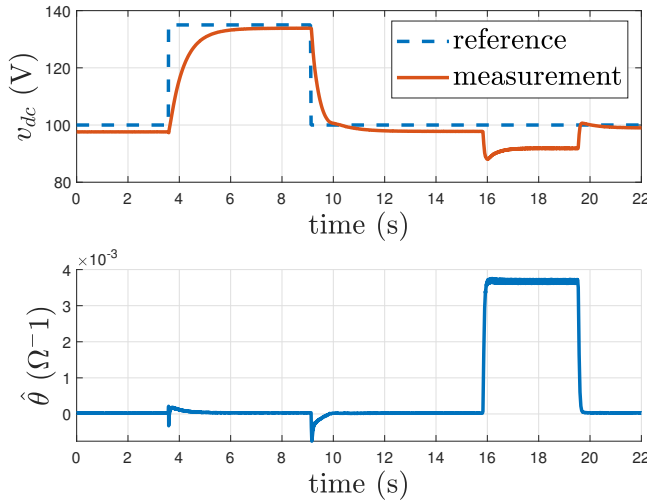


Fig. 6. Evolution of v_{dc} (upper graph) and parameter observation (lower graph) during the second experiment

During a second experimental procedure, the voltage controller is tested. The voltage controller parameter g in (19) is chosen equals to 2. The observer (17) is chosen to estimate the parameter θ and its parameter k is equals to 25. A voltage step making the reference goes from 100 V to 135 V is firstly applied. The reference is then brought back to 100 V. After this voltage control phase, a load step is applied decreasing the load R_L from $11k\Omega$ to 300Ω . The results of this second experiment are shown on Fig. 7. The voltage is regulated close to its reference even under load variation. The voltage measurement shows a slight steady-state error, this is due to the uncertainties on the experimental parameters

despite their careful determination. This steady-state error is avoidable by adding an integral term on the control law, this improvement is left for a future work. With the addition of an integral term, the stability proof is challenging. Despite the relevance of a load observer can be questioned when an integral action is added to the control law, the authors think that it remains appropriate. Indeed, the use of a load observer result in a smaller integral term. This is particularly desirable when control saturation occurs because it reduces the wind-up phenomenon.

The load perturbation is mostly but not completely rejected since the SynRM's parameters are not exactly known as explained before. A coupling effect between the observer and the voltage regulation is visible. A change in the voltage reference implies a quick transient on the load observer. This coupling effect is partly due to the voltage filtering used in order to avoid the noise on the voltage measurement. The speed regulation of the PMSM used as a prime mover also has an effect since the speed is not kept constant when the mechanical load is changed through the variation in the power recovery of the SynRM.

In a third experiment, the voltage reference is kept at 100V and the observed parameter is not provided to the voltage controller. That is, the parameter $\frac{1}{R_T}$ is no more replaced by $\hat{\theta}$ but rather by 0 in the equation (6). The resistive load effect is then not compensated. The same load step as before is applied to the system. The results are shown on the middle and lower graphs of Fig.8. The upper graph of Fig.8 comes from the voltage regulation of the second experiment. Before the load step appears, the two first graph are very similar. This is explained by the fact that the resistive load is large, meaning that $\frac{1}{R_T}$ is close to zero. In that sense considering

it as equal to zero does not imply a large error. Because the resistive load is not compensated, a large steady states error appears when it changes to a lower value. After the load step, the voltage takes more time to reach its reference when the resistive load is not compensated. The apparent benefits of the observer based controller is resumed on Fig. 8.

VII. CONCLUSION

The non-linear reduced observer proposed in this paper shows a convergence dynamic independent of the operating point of the system. This is particularly interesting for system operating in a wide range of x . The proposed observer is used in a voltage controller in order to improve the rejection of perturbations caused by a load variation. Adding an integral action in the voltage controller and theoretically verifying the stability of the overall closed loop system are considered for future works. The improvement of the experimental application is also an avenue for future works.

REFERENCES

- [1] Branko Ban, Stjepan Stipetić, and Mario Klanac. Synchronous reluctance machines: Theory, design and the potential use in traction applications. In *2019 International Conference on Electrical Drives & Power Electronics (EDPE)*, pages 177–188. IEEE, 2019.
- [2] Ion Boldea, Lucian N Tutelea, Leila Parsa, and David Dorrell. Automotive electric propulsion systems with reduced or no permanent magnets: An overview. *IEEE Transactions on Industrial Electronics*, 61(10):5696–5711, 2014.
- [3] Wen-Hua Chen, Jun Yang, Lei Guo, and Shihua Li. Disturbance-observer-based control and related methods—an overview. *IEEE Transactions on Industrial Electronics*, 63(2):1083–1095, 2015.
- [4] CM Donaghy-Spargo. Synchronous reluctance motor technology: opportunities, challenges and future direction. *Engineering & technology reference.*, pages 1–15, 2016.
- [5] Bernard Friedland. A nonlinear observer for estimating parameters in dynamic systems. *Automatica*, 33(8):1525–1530, 1997.
- [6] S Hazra and P Sensarma. Vector approach for self-excitation and control of induction machine in stand-alone wind power generation. *IET Renewable Power Generation*, 5(5):397–405, 2011.
- [7] S Hazra and PS Sensarma. Self-excitation and control of an induction generator in a stand-alone wind energy conversion system. *IET renewable power generation*, 4(4):383–393, 2010.
- [8] Thomas Jahns. Getting rare-earth magnets out of ev traction machines: A review of the many approaches being pursued to minimize or eliminate rare-earth magnets from future ev drivetrains. *IEEE Electrification Magazine*, 5(1):6–18, 2017.
- [9] Hannu Kärkkäinen, Lassi Aarniovuori, Markku Niemelä, Juha Pyrhönen, and Jere Kolehmainen. Technology comparison of induction motor and synchronous reluctance motor. In *IECON 2017-43rd Annual Conference of the IEEE Industrial Electronics Society*, pages 2207–2212. IEEE, 2017.
- [10] Subramaniam Senthil Kumar, Natarajan Kumaresan, Muthiah Subbiah, and Mahendhar Rageeru. Modelling, analysis and control of stand-alone self-excited induction generator-pulse width modulation rectifier systems feeding constant dc voltage applications. *IET Generation, Transmission & Distribution*, 8(6):1140–1155, 2014.
- [11] Dong-Choon Lee, G-Myoung Lee, and Ki-Do Lee. Dc-bus voltage control of three-phase ac/dc pwm converters using feedback linearization. *IEEE transactions on industry applications*, 36(3):826–833, 2000.
- [12] Takayoshi Matsuo and Thomas A Lipo. Field oriented control of synchronous reluctance machine. In *Proceedings of IEEE Power Electronics Specialist Conference-PESC'93*, pages 425–431. IEEE, 1993.
- [13] Paolo Mercorelli. Parameters identification in a permanent magnet three-phase synchronous motor of a city-bus for an intelligent drive assistant. *International Journal of Modelling, Identification and Control* 5, 21(4):352–361, 2014.
- [14] Z. Mynar, P. Vaclavek, and P. Blaha. Synchronous reluctance motor parameter and state estimation using extended kalman filter and current derivative measurement. *IEEE Transactions on Industrial Electronics*, 68(3):1972–1981, 2021.
- [15] Mauro Di Nardo, Giovanni Lo Calzo, Michael Galea, and Chris Gerada. Design optimization of a high-speed synchronous reluctance machine. *IEEE Transactions on Industry Applications*, 54(1):233–243, 2018.
- [16] Robert H Park. Two-reaction theory of synchronous machines generalized method of analysis-part i. *Transactions of the American Institute of Electrical Engineers*, 48(3):716–727, 1929.
- [17] Khwaja M Rahman and Silva Hiti. Identification of machine parameters of a synchronous motor. *IEEE Transactions on Industry Applications*, 41(2):557–565, 2005.
- [18] Alireza Siadatan, Mehdi Kholousi Adab, and H Kashian. Compare motors of toyota prius and synchronous reluctance for using in electric vehicle and hybrid electric vehicle. In *2017 IEEE Electrical Power and Energy Conference (EPEC)*, pages 1–6. IEEE, 2017.
- [19] Miguel Velez-Reyes, Kazuaki Minami, and George C Verghese. Recursive speed and parameter estimation for induction machines. In *Conference Record of the IEEE Industry Applications Society Annual Meeting.*, pages 607–611. IEEE, 1989.
- [20] Paul Waide and Conrad U Brunner. Energy-efficiency policy opportunities for electric motor-driven systems. 2011.
- [21] Yawei Wang, Nicola Bianchi, Silverio Bolognani, and Luigi Alberti. Synchronous motors for traction applications. In *2017 International Conference of Electrical and Electronic Technologies for Automotive*, pages 1–8. IEEE, 2017.
- [22] Wei Xu and Robert D. Lorenz. High-frequency injection-based stator flux linkage and torque estimation for db-dtfc implementation on ipmsms considering cross-saturation effects. *IEEE Transactions on Industry Applications*, 50(6):3805–3815, 2014.
- [23] Kai Zhang, Zhenyu Shan, and Juri Jatskevich. Estimating switching loss and core loss in dual active bridge dc-dc converters. In *2015 IEEE 16th Workshop on Control and Modeling for Power Electronics (COMPEL)*, pages 1–6, 2015.
- [24] Xiaoguang Zhang and Zhengxi Li. Sliding-mode observer-based mechanical parameter estimation for permanent magnet synchronous motor. *IEEE Transactions on Power Electronics*, 31(8):5732–5745, 2016.